Hindawi Publishing Corporation
Advances in Meteorology
Volume 2010, Article ID 959014, 8 pages
doi:10.1155/2010/959014

Research Article

Orography-Induced Gravity Wave Drag Parameterization in the Global WRF: Implementation and Sensitivity to Shortwave Radiation Schemes

Hyeyum Hailey Shin,[1] Song-You Hong,[1] Jimy Dudhia,[2] and Young-Joon Kim[3]

[1] *Department of Atmospheric Sciences and Global Environment Laboratory, Yonsei University, Seoul 120-749, Republic of Korea*
[2] *Mesoscale and Microscale Meteorology Division, National Center for Atmospheric Research, Boulder, CO 80305, USA*
[3] *Marine Meteorology Division, Naval Research Laboratory, Monterey, CA 93943, USA*

Correspondence should be addressed to Song-You Hong, shong@yonsei.ac.kr

Received 24 December 2009; Accepted 24 March 2010

Academic Editor: Hann-Ming Henry Juang

This paper describes the implementation of the orographic gravity wave drag (GWDO) processes induced by subgrid-scale orography in the global version of the Weather Research and Forecasting (WRF) model. The sensitivity of the model simulated climatology to the representation of shortwave radiation and the addition of the GWDO processes is investigated using the Kim-Arakawa GWDO parameterization and the Goddard, RRTMG (Rapid Radiative Transfer Model for GCMs), and Dudhia shortwave radiation schemes. This sensitivity study is a part of efforts of selecting the physics package that can be useful in applying the WRF model to global and seasonal configuration. The climatology is relatively well simulated by the global WRF; the zonal mean zonal wind and temperature structures are reasonably represented with the Kim-Arakawa GWDO scheme using the Goddard and RRTMG shortwave schemes. It is found that the impact of the shortwave radiation scheme on the modeled atmosphere is pronounced in the upper atmospheric circulations above the tropopause mainly due to the ozone heating. The scheme that excludes the ozone process suffers from a distinct cold bias in the stratosphere. Moreover, given the improper thermodynamic environment conditions by the shortwave scheme, the role of the GWDO process is found to be limited.

1. Introduction

The Weather Research and Forecasting (WRF) model has been evaluated in terms of regional modeling for both research and operational applications since it was first released in 2000. The capability of the regional WRF model is established over a wide temporal range; from short-range forecasts such as simulations of localized heavy rainfall and snowfall within a couple of days over Korea (i.e., [1, 2]), 36-h real time forecasts in the United States [3], and simulations of typhoon and hurricane that affect synoptic fields for several days (i.e., [4, 5]), to regional climate simulations of such as U.S. warm-season precipitation and East-Asia summer monsoon circulations (i.e., [6, 7]). These studies support the satisfactory performance of the WRF model in various regions over the globe.

With the verification of the regional WRF model performance, National Center for Atmospheric Research (NCAR) researchers tested the ability of the WRF model to cover the global domain. It is noticed that a global version of WRF was first developed to study atmospheres on Mars and other planets by Mark Richardson and colleagues at California Institute of Technology, and researchers in NCAR Mesoscale and Microscale Meteorology (MMM) Division extended that version of the WRF-ARW model to forecast weather on Earth (NCAR articles on 9 November 2007, available in http://www.ncar.ucar.edu/index.php/ncar/articles/weather_forecast_goes_global). The regional WRF model was extended with a latitude-longitude grid system to cover the global domain, based on the Advanced Research WRF (ARW) version 3.0 that was released in April 2008. The global WRF shares the same dynamic core with the regional WRF

except that a polar filter is applied in the global version [8]. In addition, the physics options and behavior should be examined separately from the regional configuration because the intrinsic requirements for global circulation modeling, such as higher model top, and coarser resolution require further validation.

The advancement of human knowledge continues together with increasing computing resources; the cutting-edge numerical weather prediction (NWP) and climate models, however, cannot resolve all relevant scales of atmospheric phenomena. Global numerical prediction models are typically run with horizontal resolutions that cannot capture atmospheric processes smaller than about 10–100 km. Gravity wave is an unresolved process in coarse resolution models, playing an important role in transporting momentum from source regions to regions where gravity waves are dissipated or absorbed during their propagation, producing synoptic scale body forces [9]. Palmer et al. [10] and McFarlane [11] noted that unresolved mountain gravity wave drag was one of the most critical causes of the systematic biases in seasonal simulations—excessive surface westerlies and a too cold pole—and suggested a GWDO parameterization for large-scale models. Since then, this subgrid-scale process of gravity waves has been an essential physical process that should be parameterized in global models to represent global circulations realistically. However, the global WRF, which is a spatial extension of the original regional WRF, currently does not include any orography-induced gravity wave drag (GWDO) parameterization. It is noted that the GWDO parameterization is not included in most regional models including the WRF since horizontal resolutions of regional models are considered to be sufficiently high to resolve gravity waves. Moreover, global models include much of stratosphere, whereas the model top is lower (i.e., typically lower than 50 hPa) for regional models. Thus, most regional models do not typically include the GWDO parameterization.

The purpose of this study is to describe the implementation of the GWDO parameterization based on Kim and Arakawa [12] (hereafter, KA GWDO) into the global WRF model and evaluate the performance of the model in simulating general features of the boreal winter climate with the KA GWDO. The KA GWDO includes the enhanced low-tropospheric gravity wave drag in addition to the upper-level wave breaking that is traditionally incorporated into GWDO schemes. The KA GWDO was earlier implemented into the National Centers for Environmental Prediction (NCEP) Global Spectral Model (GSM) successfully and its performance was later reported by Hong et al. [13]. The KA GWDO scheme went into operation at the NCEP global forecast system in 2000. Sensitivity of the simulated climatology to shortwave radiation schemes is also investigated in order to re-evaluate present physics options in the WRF model in global and seasonal configuration, which have been evaluated only in regional configuration. Section 2 describes the experimental setup and implementation of the KA GWDO parameterization, and results are discussed in Section 3. Concluding remarks are given in the final section.

2. Experimental Design

2.1. The Advanced Research WRF (ARW) Model. The Advanced Research WRF (ARW; [14]) is a community model designed for both research and forecasting, which is a fully compressible nonhydrostatic model with the Arakawa-C grid system. The model performs reasonably well for detailed numerical weather prediction (NWP) cases with real-data initial and boundary conditions. The WRF model became available with the global coverage starting from WRF version 3.0, which was released in April 2008. The model used in this study is a beta version of the ARW version 3.1 with the global domain. The global WRF utilizes the latitude-longitude grid system and then a polar filter is used to filter out small-scale waves and avoid the singularity problem at the poles.

2.2. Implementation of the KA GWDO Parameterization Scheme. The KA GWDO scheme [12] includes the lower-tropospheric enhancement of GWDO due to selective low-level wave breaking mainly in downstream regions with the aid of additional subgrid-scale orographic statistics: the orographic asymmetry (OA) and orographic convexity (OC). The OA measures the asymmetry and location of subgrid-scale orography relative to the model grid box and it distinguishes between the upstream and downstream regions. The OC measures how convex or sharp the subgrid-scale orography is by statistically relating the characteristics of the mountain waves to the subgrid-scale orography.

The KA GWDO parameterization is implemented in the WRF model following Hong et al. [13]; in Hong et al. [13] the reference level is determined as the larger value between the PBL height and $2\sigma_h$ following Kim and Doyle [15], where σ_h is the standard deviation of subgrid-scale terrain heights. Kim and Hong [16] demonstrated that this method in determining the reference level greatly improves the climate simulations compared with the previous method that employs the PBL height as the reference level height; we note that the new method generally elevates the reference level height. The mechanism behind the improvement is explained in Kim and Hong [16].

For utilizing the KA GWDO in the WRF model, the necessary input to the KA GWDO scheme (i.e., mean, variance, asymmetry, and convexity) is derived from a 30-arcsecond resolution topography dataset [17] for global domains with 10 min., 20 min., 30 min., 1 deg., and 2 deg. resolutions. These orographic statistics are interpolated to the model grid points using one of the five-resolution datasets in the WRF Preprocessing System (WPS); prepared statistics of a comparable resolution to model grid size are used.

2.3. Experimental Setup. Seasonal simulations are conducted for three boreal winters in December, January, and February (DJF) of 1996/1997, 1997/1998, and 1999/2000. For each winter, five ensemble runs are conducted with different initialization times of 00UTC 1–5 November to average out the unpredictable parts of the flow. Thus, one experiment

Table 1: A summary of the physics options used in the numerical experiments. "—" denotes the same option as that in the Gsw_nGWD experiment.

	GWDO	SW	LW	PBL	LSM	CPS	MPS
Gsw_nGWD	None	Goddard	RRTMG	YSUPBL	NOAH	Grell-Devenyi	WSM3
Rsw_nGWD	None	RRTMG	—	—	—	—	—
Dsw_nGWD	None	Dudhia	—	—	—	—	—
Gsw_GWD	KA GWDO	Goddard	—	—	—	—	—
Rsw_GWD	KA GWDO	RRTMG	—	—	—	—	—
Dsw_GWD	KA GWDO	Dudhia	—	—	—	—	—

consists of 15 runs. Initial conditions are forced by the NCEP-Department of Energy (DOE) (NCEP-DOE) Reanalysis II (R2) data on the $2.5^\circ \times 2.5^\circ$ global grid. The National Oceanic and Atmospheric Administration (NOAA) Optimal Interpolation Sea Surface Temperature (OISST) is used as the surface boundary conditions every 24 hours. The horizontal resolution of $1.875^\circ \times 1.875^\circ$ is used, which is comparable to the 200 km resolution along the equator. The 38-layer Eta level system is used with the model top at 10 hPa. Intervals between the adjoining vertical levels are determined not to exceed 1 km or to be comparable to 1 km.

The physics package includes the RRTMG scheme [18] for longwave radiation, the Yonsei University Planetary Boundary Layer (YSU PBL) [19] for vertical diffusion process, the Noah land surface model [20], the Grell-Devenyi ensemble scheme [21] for cumulus parameterization, and the WSM3 (WRF Single-Moment 3-class) scheme [22] for microphysics. In the YSU PBL, the vertical diffusion coefficients in the stable boundary layer (SBL) conditions are calculated as in the case of the unstable conditions; the coefficients are parabolic functions of heights as in the mixed layer, and the SBL top is determined by the bulk Richardson number. Kim and Hong [16] demonstrated that the interaction between the KA GWDO and YSU PBL processes is improved with the SBL parameterization mentioned above. For shortwave radiation, three different shortwave schemes are used to observe the sensitivity of the simulated climate associated with the GWDO to the shortwave radiation processes in the modeled atmosphere: the Goddard [23], RRTMG, and Dudhia [24] schemes. The physics options used for the numerical experiments are summarized in Table 1.

3. Results

In this study, the results are obtained from and discussed based on the composite of 3-year simulations (i.e., ensemble averages of the 15 simulations). The simulated zonal wind and temperature structures are evaluated in comparison with the reanalysis (R2) data. The shortwave process in R2 is based on Chou [25] and Chou and Lee [26], and the GWDO scheme used in the R2 is described by Alpert et al. [27]. In precipitation analysis, the daily Global Precipitation Climatology Project (GPCP) data with a $1^\circ \times 1^\circ$ spatial resolution are used for the evaluation. Hereafter, to make a clear distinction, the global WRF without the KA GWDO implementation is designated the earlier version.

3.1. Wind and Temperature Structures. Figure 1 compares the three-winter ensemble averages of the zonal-mean zonal wind and temperature structures simulated with the Goddard (Figures 1(a) and 1(d)), RRTMG (Figures 1(b) and 1(e)) and Dudhia (Figures 1(c) and 1(f)) shortwave parameterizations in the earlier version of the global WRF that includes no effect of the GWDO (denoted by Gsw_nGWD, Rsw_nGWD, and Dsw_nGWD, resp.). The contours in each figure represent the 3-year averaged fields from the 15 ensemble members, and the color shades denote their deviations from the reanalysis fields. As can be expected and as the results show, the earlier version of the global WRF cannot reasonably represent the typical boreal winter climatology. The model clearly shows the systematic errors in the simulated climatology—too cold pole and excessively strong westerlies over the northern hemisphere (cf. Figure 1), which is typical when GWDO is not included in general circulation models. There is no separation between the tropospheric subtropical jet and stratospheric polar night jet and also the polar night jet is overly strong due mainly to the lack of GWDO. The thermodynamic structure shows too strong meridional temperature gradient in balance with the improper wind structure; the simulated temperature of the Arctic polar stratosphere is almost about 40 K colder than that of the reanalysis. Thus, it is obvious that the earlier version of the global WRF has a systematic problem due to a missing critical process; that is, orographically induced gravity wave drag. Note that the three nGWD experiments are conducted in parallel with the three GWD experiments (i.e., Gsw_GWD, Rsw_GWD, and Dsw_GWD) to validate the implementation of the KA GWDO in the global WRF model, and thus the sensitivity to shortwave process schemes is not discussed for these nGWD experiments.

With the KA GWDO implemented, the global WRF is able to reproduce the general mean structures of both the zonal-mean zonal wind (Figures 2(a)–2(c)) and temperature (Figures 2(d)–2(f)) in the troposphere. All three experiments simulate the subtropical jet in the northern hemisphere with realistic intensity, which is comparable to $45\,\mathrm{m\,s^{-1}}$ of the reanalysis data, as well as the overall mean wind state of the troposphere (Figures 2(a)–2(c)). This reasonable representation of the wind fields including the mid-latitude jet in the northern troposphere is attributed to the implementation of

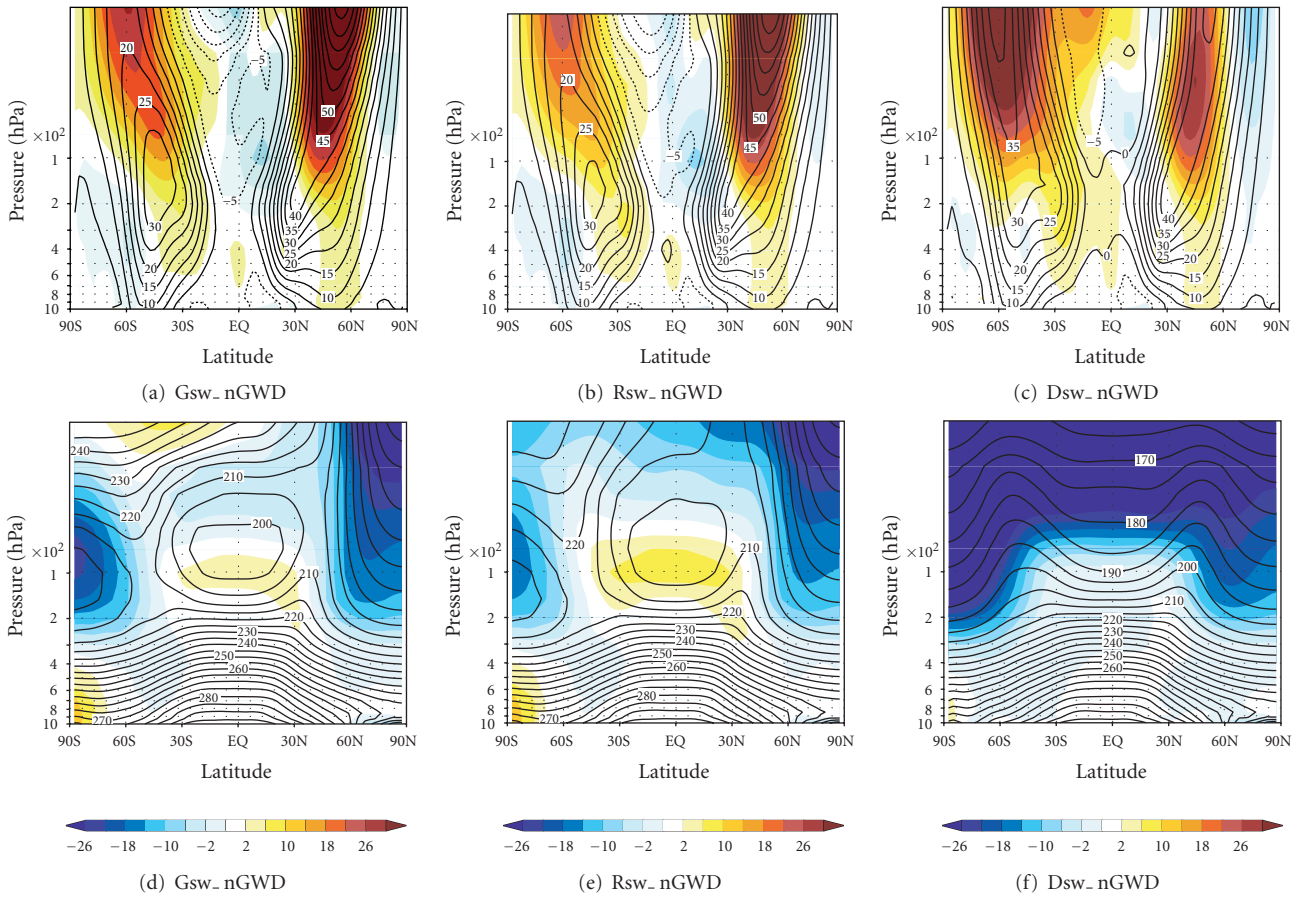

Figure 1: Three-winter ensemble averages (contours) of the zonal-mean zonal wind (upper panels) and temperature (lower panels) structures simulated from the (a), (d) Gsw_nGWD, (b), (e) Rsw_nGWD, and (c), (f) Dsw_nGWD experiments with the earlier version of global WRF without the KA GWDO implementation. Differences from the NCEP reanalysis (R2) are color shaded.

the GWDO. Associated with these improvements in the wind fields, the cold bias of the thermodynamic structures is also reduced. In the troposphere, the simulated results are less sensitive to the shortwave schemes than those in the upper atmosphere. On the other hand, clear differences among the shortwave radiation parameterizations exist in upper levels. The subtropical jet and stratospheric polar night jet in the northern hemisphere are reasonably separated with the Goddard and RRTMG shortwave radiation processes while the two jets are unrealistically bonded to each other with the Dudhia scheme; the westerly continuously decreases as the height increases such that the magnitude of the wind is evidently underestimated at the location of the observed polar-night jet, which is entirely missing in the simulation (cf. Figure 2(c)). Moreover, in the southern hemisphere, the tropospheric westerly jet is erroneously extended into the stratosphere in the Dsw_GWD experiment.

This radical difference in simulating the wind structure in the middle atmosphere among the three experiments (Gsw_GWD, Rsw_GWD, and Dsw_GWD) is related to the different thermodynamic structures that heavily rely on the shortwave heating processes. The Goddard and RRTMG shortwave schemes include ozone effects that are responsible for the typical thermodynamic structure of the stratosphere; an ozone-absorption coefficient profile is specified in the Goddard scheme according to an observed climatology, and the RRTMG scheme includes tropical/mid-latitude/polar and summer/winter ozone profiles. The simulated temperature-profile inversion near the tropical and southern-hemispheric polar tropopause is shown with these two shortwave schemes due to the ozone heating effects (Figures 2(d) and 2(e)). Because of this temperature inversion, there exists meridional temperature gradient in the middle stratosphere over high latitudes, which is responsible for the presence of the northern polar night jet in the two experiments (i.e., Gsw_GWD and Rsw_GWD). In the Gsw_nGWD and Rsw_nGWD experiments, there is significant cold bias related to the extremely overestimated temperature gradient in the lower stratospheric regions associated with the excessive westerlies caused by the missing drag, as shown previously, this cold bias is alleviated by its balance with the wind reduction due to the GWDO in the two GWD experiments.

On the other hand, the Dudhia scheme does not consider the ozone effects [28] and thus cannot simulate the temperature inversion; the strong cold bias is induced throughout

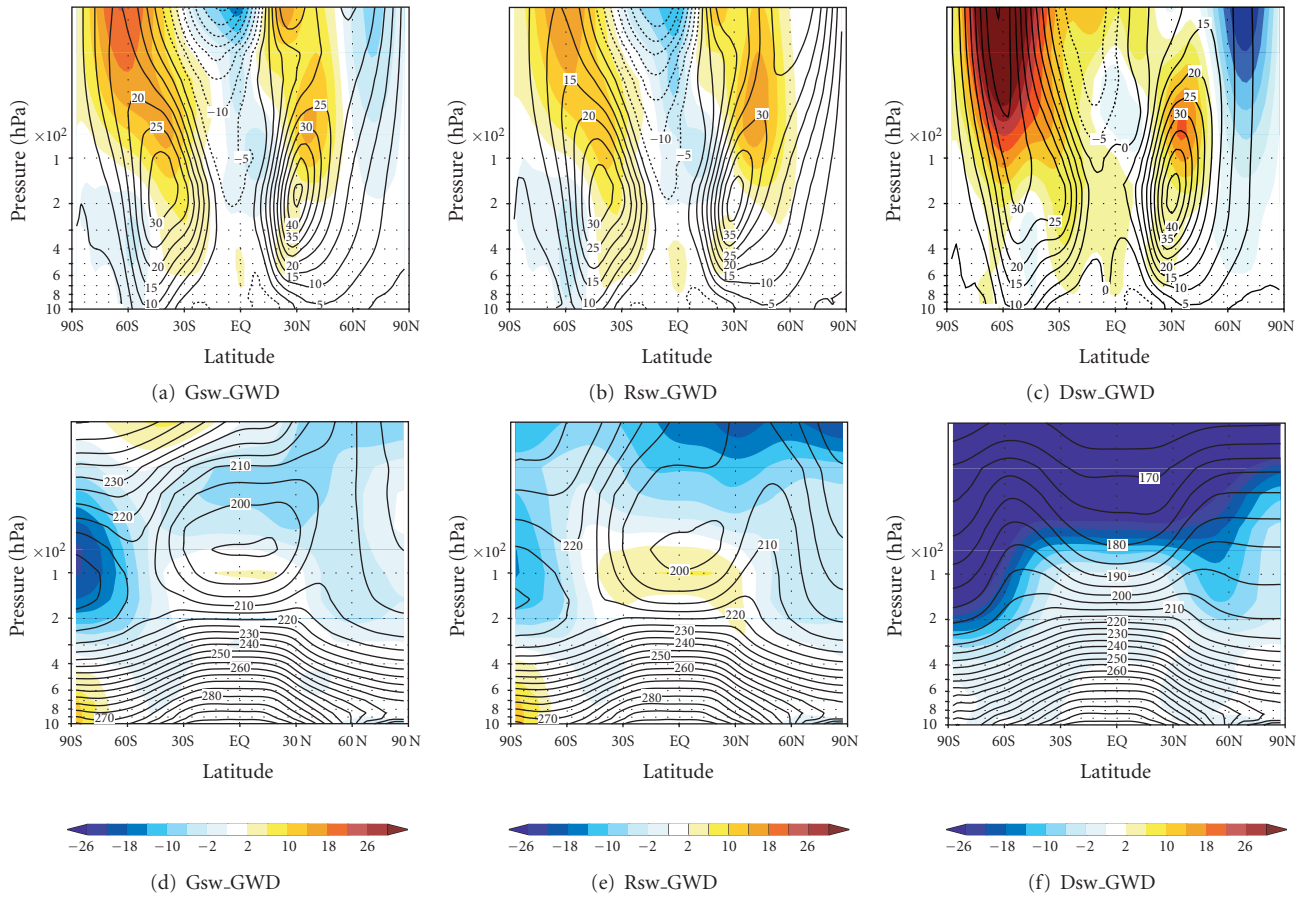

Figure 2: As in Figure 1, but with the new version of global WRF including the KA GWDO parameterization.

the stratosphere (Figure 2(f)) (note that the cold bias in the Dsw_nGWD experiment is due to the absence of both the ozone heating and GWDO). Moreover, given the highly-unrealistic thermodynamic structure, the GWDO process does not improve but continues to force the unrealistic system. We note that similar results were previously reported by Kim et al. [29]. They demonstrated that the underestimated ozone mixing ratio inducing an underestimation of shortwave heating can result in significant bias in zonal-mean temperature and wind structures; the impact of the low ozone mixing ratio is the largest in the lower polar stratosphere, which leads to the overly strong polar night jet in the northern hemisphere and unrealistically strong extension of the tropospheric westerly jet into the stratosphere in the southern hemisphere. Consequently, when the GWDO parameterization is given wrong information from other physical process, including GWDO does not improve the simulated results even though the GWDO process itself is a critical component in climate models. The Dudhia shortwave scheme shows good performance, that is, without large systematic bias, in regional weather prediction models since the model top is usually lower than 50 hPa in the regional model application, so that the simulated results do not suffer from the absent ozone effects.

In summary, shortwave radiation significantly impacts the modeled atmosphere, especially on the upper atmospheric circulations above the tropopause mainly due to the ozone heating. The heating scheme without the ozone process undergoes a distinct cold bias in the stratosphere, which in turn results in improper wind fields balancing with the cold bias. Under the unreasonable environmental conditions, the GWDO process continuously forces the system toward an unrealistic state.

3.2. Tropical Precipitation. In Figure 3, the simulated 3-year mean daily precipitation is compared with the daily GPCP data with a $1^\circ \times 1^\circ$ spatial resolution. The pattern correlation (PC), biases, and Root Mean Square Error (RMSE) between each simulation and GPCP data are presented at the top of each panel. The overall performance of the global WRF model in simulating the precipitation is acceptable in the three GWD experiments regardless of the shortwave processes (e.g., Figures 3(e)–3(g)). As seen in Shimpo et al. [30], the distribution of global precipitation from the global WRF is comparable, even though the integration period differs from one to another. The model produces tropical rainfall distributions quite reasonably, compared with the observations showing the double rainbelts along the double intertropical convergence zone (ITCZ) and precipitation

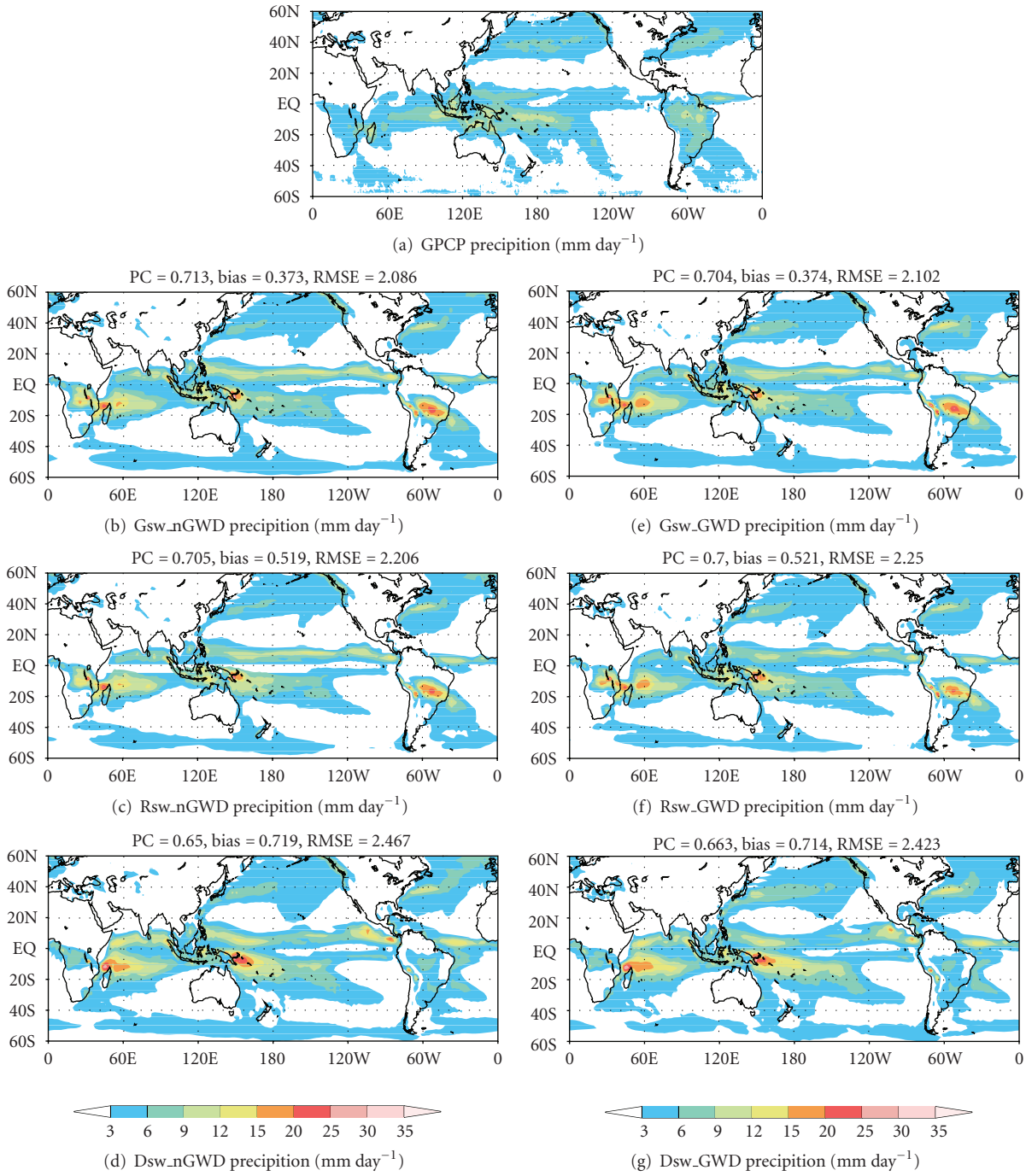

Figure 3: Comparison of 3-year averaged daily precipitation (mm day^{-1}) obtained from (a) observations, (b), (c), (d) the experiments without the KA GWDO scheme and with three different shortwave radiation processes, and (e), (f), (g) the experiments including the KA GWDO scheme and with three different shortwave radiation processes.

maximum regions over South America and South Africa. However, the model generally tends to overestimate the local rainfall maximum values over tropical regions (e.g., central South America, the northwestern ocean of Madagascar, near Sumatra, and western equatorial Pacific near the maritime continent), while it underestimates the rainfall around middle latitudes. Compared with the nGWD experiments, the inclusion of the GWDO neither significantly changes the distribution, nor improves the distribution of the precipitation. With the Goddard and RRTMG shortwave processes the statistics are slightly worse in the GWD experiments while the GWD experiment shows slightly better statistics with the Dudhia shortwave. The simulated hydroclimate shows the best results—although not significant—with the Goddard shortwave scheme in this study both with and without GWDO.

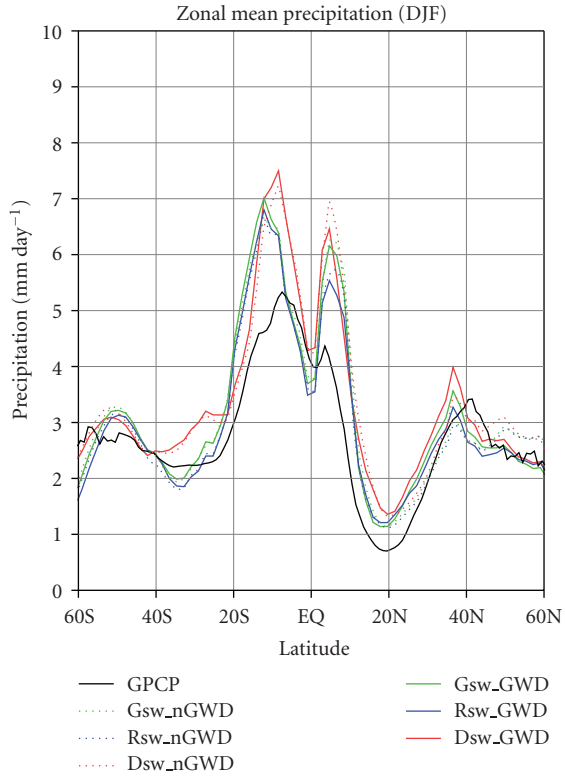

Figure 4: The zonal-mean of the 3-year mean daily precipitation (mm day^{-1}) obtained from the three nGWD (dotted lines) and three GWD (solid lines) experiments with the Goddard (green lines), RRTMG (blue lines), and Dudhia (red lines) shortwave radiation schemes, respectively.

Figure 4 shows the zonal mean of the 3-year mean daily precipitation from 60°S to 60°N. The model is successful in representing meridional distributions of the zonal-mean precipitation, but tends to overestimate the precipitation over the tropics, regardless of the shortwave scheme. Near the equator, the simulated daily precipitation patterns from the experiments with the shortwave schemes including ozone effects (i.e., the Goddard and RRTMG) are similar to each other while the experiment with the Dudhia scheme shows somewhat different behaviors, both with and without the KA GWDO. In other words, the experiments with the Goddard and RRTMG schemes commonly produce less rainfall than the experiment with the Dudhia scheme so that the amounts are closer to observations than that with the Dudhia scheme.

4. Concluding Remarks

The orographic gravity-wave drag (GWDO) process induced by subgrid scale orography is implemented in the global version of Weather Research and Forecasting (WRF) model. The sensitivity of the simulated climatology to the representation of shortwave radiation with the GWDO process in the modeled atmosphere is investigated using the Kim-Arakawa GWDO (KA GWDO) parameterization and the Goddard, RRTMG, and Dudhia shortwave radiation schemes.

With the KA GWDO parameterization implemented, the climatology from the global WRF is relatively well simulated in the troposphere; the zonal-mean zonal wind and temperature structures are realistically represented. In the stratosphere, however, the performance of the model widely varies according to the representations of shortwave processes mainly due to the ozone heating. The scheme that excludes the ozone process induces a distinct cold bias in the stratosphere, and modeled wind fields balance with the unreasonable thermodynamic fields. The already unrealistic system due to the deficiency in the heating scheme is continuously impelled by the GWDO process. This result supports the notion that the success of a particular physics parameterization scheme in atmospheric models depends not only on the accuracy of the particular scheme itself but also on the success of other physical processes [16]. In view of the precipitation, the global WRF also well represents the overall patterns of the tropical precipitation but the model tends to overestimate (underestimate) the precipitation at the tropical (mid-latitude) regions. It is found that the simulated meridional precipitation distributions differ according to the shortwave schemes depending on the presence of ozone effects.

The KA GWDO is implemented in the WRF model based on this study and became available starting from the WRF version 3.1, which was released in April 2009.

Acknowledgments

This paper was supported by the Basic Science Research Program through the National Research Foundation of Korea (NRF) funded by the Ministry of Education, Science and Technology (2010-0000840), and by the Korean Foundation for International Cooperation Science & Technology (KICOS) 21 through a grant provided by the Korean Ministry of Science & Technology (MOST).

References

[1] S.-Y. Hong and J.-W. Lee, "Assessment of the WRF model in reproducing a flash-flood heavy rainfall event over Korea," *Atmospheric Research*, vol. 93, no. 4, pp. 818–831, 2009.

[2] K.-S. Lim and S.-Y. Hong, "Numerical simulation of heavy snowfall over the Ho-Nam province of Korea in December 2005," *Journal of the Korean Meteorological Society*, vol. 43, no. 2, pp. 161–173, 2007.

[3] M. L. Weisman, C. Davis, W. Wang, K. W. Manning, and J. B. Klemp, "Experiences with 0-36-h explicit convective forecasts with the WRF-ARW model," *Weather and Forecasting*, vol. 23, no. 3, pp. 407–437, 2008.

[4] G. Jianfeng, Q. Xiao, Y.-H. Kuo, D. M. Barker, X. Jishan, and M. Xiaoxing, "Assimilation and simulation of typhoon Rusa (2002) using the WRF system," *Advances in Atmospheric Sciences*, vol. 22, no. 3, pp. 415–427, 2005.

[5] X. Li and Z. Pu, "Sensitivity of numerical simulation of early rapid intensification of Hurricane Emily (2005) to cloud

microphysical and planetary boundary layer parameterizations," *Monthly Weather Review*, vol. 136, no. 12, pp. 4819–4838, 2008.

[6] M. S. Bukovsky and D. J. Karoly, "Precipitation simulations using WRF as a nested regional climate model," *Journal of Applied Meteorology and Climatology*, vol. 48, no. 10, pp. 2152–2159, 2009.

[7] S.-R. Ham, S.-J. Park, C.-H. Bang, B.-J. Jung, and S.-Y. Hong, "Intercomparison of the East-Asian summer monsoon on 11-18 July 2004, simulated by WRF, MM5, and RSM models," *Atmosphere*, vol. 15, no. 2, pp. 91–99, 2005.

[8] W.-C. Skamarock, "Global WRF development," in *Proceedings of the 9th WRF User's Workshop*, Boulder, Colo, USA, June 2008.

[9] Y.-J. Kim, S. D. Eckermann, and H.-Y. Chun, "An overview of the past, present and future of gravity-wave drag parametrization for numerical climate and weather prediction models," *Atmosphere-Ocean*, vol. 41, no. 1, pp. 65–98, 2003.

[10] T. N. Palmer, G. J. Shutts, and R. Swinbank, "Alleviation of a systematic westerly bias in general circulation and numerical weather prediction models through an orographic gravity wave drag parameterization," *Quarterly Journal of the Royal Meteorological Society*, vol. 112, no. 474, pp. 1001–1039, 1986.

[11] N. A. McFarlane, "The effect of orographically excited gravity wave drag on the general circulation of the lower stratosphere and troposphere," *Journal of the Atmospheric Sciences*, vol. 44, no. 14, pp. 1775–1800, 1987.

[12] Y.-J. Kim and A. Arakawa, "Improvement of orographic gravity wave parameterization using a mesoscale gravity wave model," *Journal of the Atmospheric Sciences*, vol. 52, no. 11, pp. 1875–1902, 1995.

[13] S.-Y. Hong, J. Choi, E.-C. Chang, H. Park, and Y.-J. Kim, "Lower-tropospheric enhancement of gravity wave drag in a global spectral atmospheric forecast model," *Weather and Forecasting*, vol. 23, no. 3, pp. 523–531, 2008.

[14] W. C. Skamarock, J.-B. Klemp, J. Dudhia, et al., "A description of the advanced research WRF version 3," Tech. Rep. NCAR/TN-475+STR, 2008.

[15] Y.-J. Kim and J. D. Doyle, "Extension of an orographic-drag parametrization scheme to incorporate orographic anisotropy and flow blocking," *Quarterly Journal of the Royal Meteorological Society*, vol. 131, no. 609, pp. 1893–1921, 2005.

[16] Y.-J. Kim and S.-Y. Hong, "Interaction between the orography-induced gravity wave drag and boundary layer processes in a global atmospheric model," *Geophysical Research Letters*, vol. 36, Article ID L12809, 2009.

[17] S.-Y. Hong, "New global orography data sets," Office Note 424, NCEP, Camp Springs, Md, USA, 1999.

[18] E. J. Mlawer, S. J. Taubman, P. D. Brown, M. J. Iacono, and S. A. Clough, "Radiative transfer for inhomogeneous atmospheres: RRTM, a validated correlated-k model for the longwave," *Journal of Geophysical Research*, vol. 102, no. 14, pp. 16663–16682, 1997.

[19] S.-Y. Hong, Y. Noh, and J. Dudhia, "A new vertical diffusion package with an explicit treatment of entrainment processes," *Monthly Weather Review*, vol. 134, no. 9, pp. 2318–2341, 2006.

[20] F. Chen and J. Dudhia, "Coupling and advanced land surface-hydrology model with the Penn State-NCAR MM5 modeling system. Part I: model implementation and sensitivity," *Monthly Weather Review*, vol. 129, no. 4, pp. 569–585, 2001.

[21] G. A. Grell and D. Dévényi, "A generalized approach to parameterizing convection combining ensemble and data assimilation techniques," *Geophysical Research Letters*, vol. 29, no. 14, 1693, 2002.

[22] S.-Y. Hong, J. Dudhia, and S.-H. Chen, "A revised approach to ice microphysical processes for the bulk parameterization of clouds and precipitation," *Monthly Weather Review*, vol. 132, no. 1, pp. 103–120, 2004.

[23] M.-D. Chou and M. J. Suarez, "A solar radiation parameterization for atmospheric studies," Technical Report Series on Global Modeling and Data Assimilation 104606, 1999.

[24] J. Dudhia, "Numerical study of convection observed during the winter monsoon experiment using a mesoscale two-dimensional model," *Journal of the Atmospheric Sciences*, vol. 46, no. 20, pp. 3077–3107, 1989.

[25] M.-D. Chou, "A solar radiation model for use in climate studies," *Journal of the Atmospheric Sciences*, vol. 49, no. 9, pp. 762–772, 1992.

[26] M.-D. Chou and K.-T. Lee, "Parameterizations for the absorption of solar radiation by water vapor and ozone," *Journal of the Atmospheric Sciences*, vol. 53, no. 8, pp. 1203–1208, 1996.

[27] J. C. Alpert, M. Kanamitsu, P. M. Caplan, J. G. Sela, G. H. White, and E. Kalnay, "Mountain induced gravity wave drag parameterization in the NMC medium-range forecast model," in *Proceedings of the 8th Conference on Numerical Weather Prediction*, pp. 726–733, American Meteorological Society, Baltimore, Md, USA, 1988.

[28] R. J. Zamora, S. Solomon, E. G. Dutton, et al., "Comparing MM5 radiative fluxes with observations gathered during the 1995 and 1999 Nashville southern oxidants studies," *Journal of Geophysical Research*, vol. 108, no. D2, 4050, 2003.

[29] Y.-J. Kim, J. D. Farrara, and C. R. Mechoso, "Sensitivity of AGCM simulations to modifications in the ozone distribution and refinements in selected physical parameterizations," *Journal of the Meteorological Society of Japan*, vol. 76, no. 5, pp. 695–709, 1998.

[30] A. Shimpo, M. Kanamitsu, S. F. Iacobellis, and S.-Y. Hong, "Comparison of four cloud schemes in simulating the seasonal mean field forced by the observed sea surface temperature," *Monthly Weather Review*, vol. 136, no. 7, pp. 2557–2575, 2008.